Dynamically Amorphous Character of Electronic States in Poly(dA)−Poly(dT) DNA

ARTICLE *in* THE JOURNAL OF PHYSICAL CHEMISTRY B · FEBRUARY 2003

Impact Factor: 3.3 · DOI: 10.1021/jp026772u

Dynamically Amorphous Character of Electronic States in Poly(dA)−Poly(dT) DNA

James P. Lewis,*,† Thomas E. Cheatham, III,‡ Eugene B. Starikov,§ Hao Wang,|| and Otto F. Sankey||

Department of Physics and Astronomy, Brigham Young University, N233 ESC P.O. Box 24658, Provo, Utah 84602-4658, Departments of Medicinal Chemistry and of Pharmaceutics and Pharmaceutical Chemistry, University of Utah, 30 South 2000 East, Room 201, Salt Lake City, Utah 84112-5820, Karolinska Institutet Department of Biosciences at NOVUM Center for Structural Biochemistry, S-141 57 Huddinge, Sweden and Institute for Crystallography, Free University of Berlin, Takustr. 6 D-14195 Berlin, Germany, and Department of Physics and Astronomy, Arizona State University, Tempe, Arizona 85217-1504

Received: August 15, 2002; In Final Form: January 2, 2003

We present theoretical work on the electronic states in a model DNA double helix of poly(dA)−poly(dT) (10 base pairs) as the molecule undergoes thermal fluctuations at room temperature. We couple state-of-the art empirical force field molecular dynamics (MD) simulations with an ab initio tight-binding formalism based on density-functional theory [Lewis et al. *Phys. Rev. B* **2001**, *64*, 195103−1]. The dynamical features of the charge density distributions and the electronic structure are presented. The periodic structure exhibits extended HOMO−LUMO electronic states; however, equivalent states are quite localized in the aperiodic structures generated as snapshots from the MD simulation. Our results show strong Anderson localization in DNA as a result of the disorder due to structural changes promoted by the thermal fluctuations.

1. Introduction

The mechanisms of electron or hole transport in deoxyribonucleic acid (DNA) have been examined intensely within the past few years. Fundamental attempts to answer questions have generated debate as to whether DNA is an insulator, a semiconductor, a metal, or a superconductor. Pioneering experiments have produced different interpretations and lively discussion.[1−8] The latter interest is driven by DNA's supreme importance in biology and life as carriers of genetical information. Also, charge migration is critical in oxidation and reduction processes related to DNA radiational biology, and there is recent interest in DNA as the active element in potential molecular electronics devices. This last proposal is especially attractive, since advanced synthetic methods exist that produce, on-demand, a wide variety of complex DNA sequences and structures.

There are highly contradictory issues concerning long-range charge transfer along nucleic acid polymers. Resolution of these issues bears a profound technological significance for nucleic acid nanotechnology, as well as for creating new hybrid DNA−polymer materials (see, for example, refs 9 and 10). Of course, charge transfer in DNA has possible biological and physiological importance, for example, in connection with DNA repair of oxidative damage, see for example, refs 11−14). There are proposals concerning the therapeutic significance of DNA charge transfer,[15] including the repair of well-known[16,17] mutagenic photolesions in DNA (cis-syn-thymine [2+2] photodimers), although such proposals are vigorously debated.[18]

DNA charge-transfer experiments are devoted to two main physicochemical aspects: (i) intrinsic conductivity and photoconductivity and (ii) induced conductivity of nucleic acids. Measuring the intrinsic conductivity and photoconductivity of nucleic acids is a mature[19] but still challenging proposal since nucleic acids appear to conduct electrical current comparably to conventional conjugated polymers such as polyacetylene.[4,20] Similarly, measuring the induced conductivity of nucleic acids can be performed in a variety of ways;[21,22] however, despite Herculean efforts, a complete understanding of the mechanisms of charge transfer through DNA remains a challenge.[23,24] A debatable issue is whether DNA double helices can be considered as molecular wires or not. The problem is whether DNA charge transfer has a long-range or short-range nature, as several experiments and simulations observe both mechanisms.[25−28] The notion of a molecular wire seems to apply to the DNA double helix because of its unique π-electron system of bases stacked upon each other. At first glance this is reminiscent of certain charge-transfer molecular metals such as TTF−TCNQ. Moreover, this speculation is vivid, since, as mentioned earlier, the nature of base interactions within the stacks is not yet completely understood.

To analyze the experimental data on DNA charge transfer, one conventionally uses Markus-Levich-Jortner theory of charge transfer,[29] which has proven to be successful for various charge transfer processes including those in proteins. According to Markus theory, an electronic mixing is required between the initial (donor) and final (acceptor) states. In most intra- and intermolecular charge transfer reactions of (bio)organic chemistry, the charge is localized only on the initial and final states, so that coherent (superexchange or tunneling) transfer applies. Intermediate (bridge) states are off resonant (higher or lower in energy than the donor and acceptor states). This produces a transfer rate that is exponentially dependent on the distance between the donor and acceptor. If the bridge states are close in energy to each other and to the donor and acceptor states,

* Corresponding author.
† Brigham Young University.
‡ University of Utah.
§ NOVUM Center for Structural Biochemistry and Free University of Berlin.
|| Arizona State University.

10.1021/jp026772u CCC: $25.00
Published on Web 02/21/2003

the charge may be trapped along its way, so that its transfer occurs by hopping, producing random walk. Hopping transport becomes more important at higher temperatures. In many cases a single-step superexchange does not adequately describe the relevant experimental data, whereas a multistep hopping does.[30,31] For example, if the number of AT bases between GC bases is less than 3−5, the main mechanism for charge hopping is superexchange,[6] but for longer AT bridges between GC bases thermal activation becomes important.

When applying the above theoretical considerations to DNA charge-transfer experiments, one must also take into account the dynamics of the DNA structure, as a few experiments[32,33] have shown. Specifically, DNA conformations vary with time as a result of a rich palette of DNA dynamical motions which occur from femtosecond to second time scales.[34] The efficiency of charge transfer (or degree of its coherence) is then determined by the comparability (or noncomparability) between the time scales of charge donor/acceptor dynamics within DNA and of DNA dynamics itself. This dynamical factor seems to be as significant as important static conditions[35] such as variations in DNA sequence and donor/acceptor-DNA binding mode. As the most recent ab initio HF−SCF calculations on the dependence of electronic matrix elements for hole transfer on conformational changes in DNA dimer duplexes show,[8] thermal fluctuations of the DNA structure have to be taken into account when one aims at a realistic description of the electron/hole transfer in DNA.

With the increase in computational power, great effort has been made by the electronic-structure community to optimize the performance of quantum mechanical methods. Calculating larger systems without making stringent approximations has only been possible within the past few years. Quantum mechanical methods are a complementary tool to experimental research. Within a density functional based local orbital tight-binding-like formalism, more complex problems can be investigated with a modest decrease in the accuracy. This is particularly useful where a quantum mechanical description is important to the investigated system's fundamental chemistry, yet where a smaller model system would inadequately describe the proper physical environment.

Here, we marry classical molecular dynamics simulations with an electronic structure density-functional method to theoretically investigate the electronic states of model DNA structures as the molecule undergoes classical thermal motion at room temperature. We investigate the dynamics of the DNA structure and its impact on the electronic structure. A similar approach was recently used to postulate the charge migration mechanism in DNA, with injected charges being gated in a concerted manner by thermal motions of hydrated counterions.[36] Here we study a longer oligonucleotide duplex than has been studied previously and demonstrate with the complete system that its electronic states dynamically localize. The mechanism is an Anderson off-diagonal dynamic disorder model similar to the static disorder that leads to localized band-tail states in amorphous semiconductors.[37−40] The concept of static Anderson localization in DNA has previously been considered by Ladik.[41,42] We show that localization in DNA reaches far deeper in energy than just bandtail states. We demonstrate for the first time this effect in a poly(dA)−poly(dT) 10-base-pair fragment; this represents one complete turn of the B-DNA double helix.

2. Computational Method

We evaluated a series of snapshots (separated by 0.5 ps) from nanosecond molecular dynamics (MD) simulations. A single-point calculation of the DNA structure of each snapshot was performed using a local-orbital method based on density functional theory (DFT) and separable pseudopotentials (called FIREBALL).[43] All poly(dA)−poly(dT) DNA atoms, including phosphate groups and backbone atoms are included in the single-point calculations which contained 10 base pairs (644 atoms). Although water and cation atoms are included in the MD simulations, they were not explicitly included in the electronic structure at this stage due to computational contraints. Adding water and cation atoms to more correctly represent the environment surrounding the DNA molecule will be the subject of future work. Hydrogen atoms are placed equidistant between the two oxygen atoms on each phosphate group for charge neutralization in the DNA molecule.

2.1. Methodology: Generating the Aperiodic Poly(dA)−Poly(dT) DNA Structures. In this paper, we consider thermal fluctuations of a poly(dA)−poly(dT) DNA 10-mer duplex fragment at room temperature from classical MD simulations; therefore, aperiodic structures of DNA are generated throughout the simulation. With our local-orbital density functional method, we compare the electronic states of an idealized model periodic canonical B-DNA poly(dA)−poly(dT) DNA structure with those thermally distorted aperiodic poly(dA)−poly(dT) DNA structures generated from the MD simulation.

Canonical B-DNA 10-base-pair models of poly(dA)−poly(dT) were built into a Arnott B-DNA[44] model using the nucgen DNA builder contained within AMBER 5.0.[45] Classical molecular dynamics trajectories of the B-DNA models, including explicit water and sodium counterions, were generated using the CHARMM (version c26n1).[46] Both models were solvated with enough preequilibrated TIPSP[46] water to add 12.0 Å to the maximal distance extent of the DNA. Net-neutralizing Na^+ ions[47] were placed off the phosphate oxygen bisector and then minimized (with larger, 5.0, van der Waals radii) in-vacuo prior to solvating the system. Equilibration involved the application of harmonic positional restraints (25.0 kcal/mol^{-2}) and 250 steps of ABNR minimization, followed by 25 ps of MD, where the temperature was ramped up from 50 to 300 K in 1 ps intervals. The initial equilibration was performed with the Cornell et al. force field.[48] Subsequent equilibration with the BMS force field of Langley[49] involved 250 steps of ABNR minimization followed by 5 ps of MD with position restraints.

All production simulations were performed without any restraints and the BMS force field of Langley. Production simulation was performed for 10 nanoseconds with CHARMM (version c26n1)[46] in a consistent manner. This involved constant temperature (300 K, mass = 1000)[50] and pressure (1 atm, piston mass = 500 amu, relaxation time = 20 ps^{-1}),[51] 2 fs time steps with the application of SHAKE[52] on hydrogen atoms, accurate use of the particle mesh Ewald method[53] (∼1.0 grid size with 6th order B-spline interpolation and a Ewald coefficient of 0.34) in rhombic dodecahedral unit cells ($x = y = z$, $\alpha = 60°$, $\beta = 90°$, $\gamma = 60°$), a heuristically updated atom based pairlist built to 12.0 Å and cutoff at 10.0 Å with a smooth shift of the van der Waals energies. These methods have proven reliable for representing DNA duplex structure[54,55] and the BMS force field very accurately models B-DNA crystal structures.[49,56]

2.2. Theoretical Basis of the FIREBALL Method. The theoretical basis of the FIREBALL method is the use of DFT with a nonlocal pseudopotential scheme. A summary of the method will be given here, and we refer the reader to ref 43 and references therein for a more detailed description of the method.

At the core of the method is the replacement of the Kohn−Sham energy functional by the approximate Harris−Foulkes functional:[57,58]

$$E_{\mathrm{tot}}^{\mathrm{Harris}} = E^{\mathrm{BS}} + \{U^{\mathrm{ion-ion}} - U^{\mathrm{ee}}[\rho_{\mathrm{in}}(\mathbf{r})]\} + \{U^{\mathrm{xc}}[\rho_{\mathrm{in}}(\mathbf{r})] - V^{\mathrm{xc}}[\rho_{\mathrm{in}}(\mathbf{r})]\} \quad (1)$$

The main difference between the Kohn−Sham and Harris−Foulkes functional is that the latter is defined entirely in terms of an input charge density, $\rho_{\mathrm{in}}(\mathbf{r})$; whereas, the former is defined in terms of both an input and output charge density and the two converge when self-consistency is used. In eq 1, E^{BS} is the band structure energy ($2\sum_{i\epsilon \mathrm{occ}}\epsilon_i$), where ϵ_i are the eigenvalues of the one-electron Schrödinger equation. The second term of eq 1 is the "short-range" repulsive interaction which is the ion−ion interaction offset by the overcounting of the Hartree interactions; the last term is a correction to the exchange-correlation. In this work, we use the Becke (B88) form for the exchange interactions[59] with the Lee−Yang−Parr (LYP) form for the correlation interactions.[60] The Harris functional forms the basis of our method; however, we include charge transfer between atoms self-consistently by extending the Harris functional to second order in a variation in the charge density.[61]

In solving the one-electron Schrödinger equation, a set of slightly excited pseudoatomic "fireball" wave functions are used. These orbitals are computed within DFT and a norm-conserving separable pseudopotential[62] and are chosen such that they vanish at some radius r_c ($\psi^{\mathrm{atomic}}_{\mathrm{fireball}|r\geq r_c} = 0$). This boundary condition is equivalent to an "atom in the box" and has the effect of raising the electronic energy levels (ϵ_s, ϵ_p, ϵ_d, ... atomic eigenvalues) due to confinement. The radial cutoffs (r_c) are chosen such that these electronic eigenvalues remain negative and are mildly perturbed from the free atom. The "fireball" boundary condition yields two promising features. First, the range of matrix elements between orbitals on different atoms is limited; therefore, very sparse matrices are created for large systems. This inherent sparseness allows one to more readily implement linear-scaling algorithms to obtain the band structure energy. Second, the slight excitation of the atoms somewhat accounts for Fermi compression in solids, which apparently gives a better representation of solid-state charge densities.[63] For this work, we choose a minimal basis set for H, C, N, and P, and a double numerical basis on O. Oxygen atoms on the phosphate groups require additional flexibility in order to generate the correct charge polarization.

2.3. Quantifying the Degree of Localization. The phenomena of Anderson localization[37] refers to the localization of mobile quantum mechanical entities, such as spin or electrons, due to impurities, spin diffusion, or randomness. Anderson localization applied to DNA may come from two distinct mechanisms: diagonal or off-diagonal disorder. Diagonal disorder induced localization occurs from variations of the sequence along the base stack, and off-diagonal disorder occurs by variations either from bonding between bases along the stack or from hydrogen bonding variations across the double helix. The qualitative physics of localization is described by an Anderson model,

$$H = \sum_i \epsilon_i c_i^{\dagger} c_i + \sum_{i,j}{}' t_{i,j} c_i^{\dagger} c_j + t_{j,i} c_j^{\dagger} c_i \quad (2)$$

where each molecular orbital $(\mathrm{MO})_i$ of a base has energy ϵ_i and interacts with its nearest neighbor base MO_j ($i \neq j$) with a Hamiltonian hopping interaction of t_{ij}. The Anderson model of diagonal disorder randomly varies the on-site Hamiltonian matrix elements (diagonal) ϵ_i and describes the A−T−G−C random sequencing of DNA.

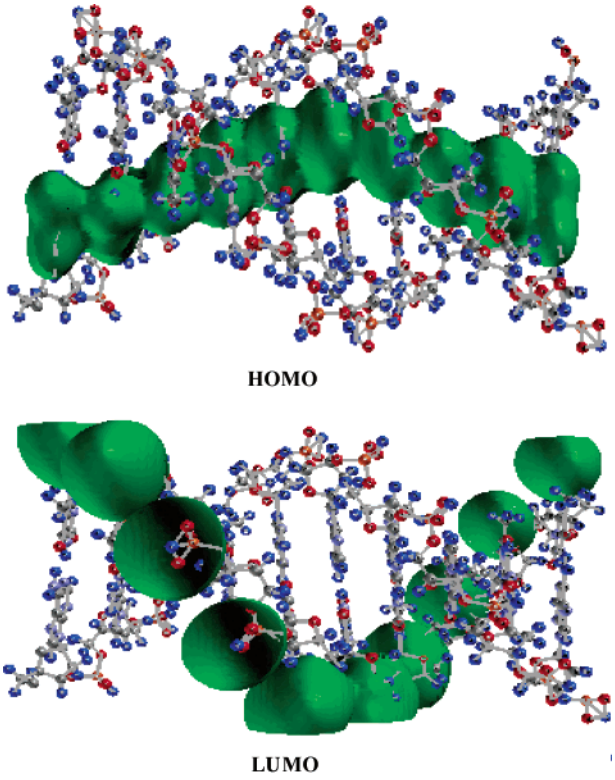

Figure 1. Population densities for the highest occupied molecular orbital (HOMO) and the lowest unoccupied molecular orbital (LUMO) are shown for periodic poly(dA)−poly(dT) DNA (10 base pairs). Both molecular orbitals exhibit very extended and periodic (Bloch-like) states throughout the molecule.

In this paper we focus on B-DNA structures of poly(dA)−poly(dT) in which there exists only one base pair combination A−T; each strand has only a single type of base in its stack. In this system, only off-diagonal disorder may occur. The bonds within a single base are strong, but thermal fluctuations coupled with weak π-bonding occurs along the stack, and the weak hydrogen bonds across the strands of the DNA double helix allow individual bases significant freedom of movement, including transient base pair opening and DNA breathing events over millisecond time scales[64] and large fluctuations in the structure.[65] Stochastic fluctuations of the weak bonding modulates the electronic coupling, t_{ij}, between adjacent bases. If the dynamic fluctuations of t_{ij} are large enough, localized electronic states are produced as in an amorphous solid.

We quantify the spatial extent of an electronic state by defining the number of accessible atoms, W, from the electronic state quantum entropy. From a particular state ν, the wave function $\psi(\nu)$ has a Mulliken population $p_i(\nu)$ on atom i, which loosely is considered the probability that an electron in state ν and resides on a particular atom i. The populations are normalized, $\sum_i p_i(\nu) = 1$. From probability theory, we define a quantum entropy for state ν as

$$S(\nu) = -\sum_i p_i(\nu) \ln p_i(\nu)$$

For example, a state ν with equal probabilities over N_0 atoms ($N_0 \leq N_{\mathrm{total}}$), gives an entropy of $\ln N_0$. From Boltzmann's equation, we can determine the number of accessible atoms $W(\nu)$ for electronic state ν as $S(\nu) = \ln W(\nu)$, or $W(\nu) = e^{S(\nu)}$. Our

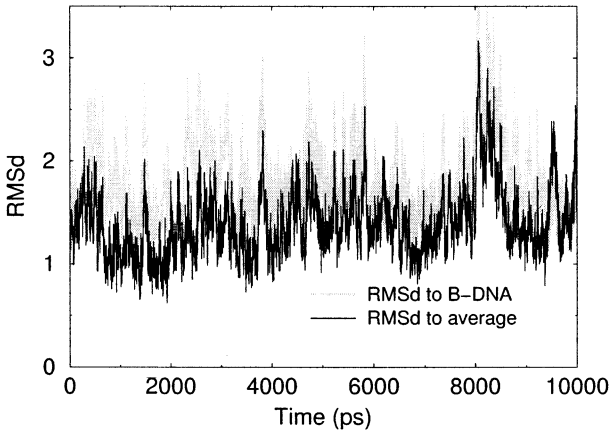

Figure 2. Shown in black and gray are the all-atom best-fit root-mean-squared deviations (in Å) as a function of time compared to canonical B-DNA (gray) and the straight coordinate average structure from the 1.5−2.5 ns portion of the trajectory (at 0.5 ps intervals).

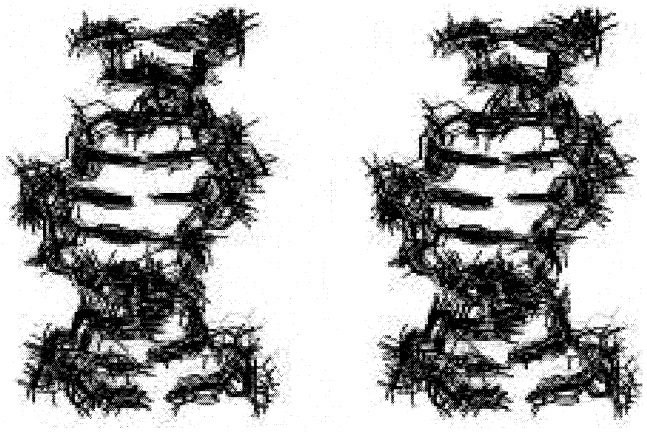

Figure 3. Shown in walleye stereo are representative configurations (closest to the centroid) from each of 10 clusters obtained by hierarchical clustering (with a pairwise RMSd metric) of the 200 equally spaced configurations from 1.5 to 2.5 ns.

example state with equal probabilities spread over N_0 atoms gives the expected result, $W(\nu) = N_0$. For the complex electronic states of DNA, the number of accessible atoms $W(\nu)$ gives a quantitative, and easily calculable, measure for how many atoms a particular electronic state $\psi(\nu)$ reaches.

3. Results

3.1. Electronic States of a Periodic Poly(dA)−Poly(dT) DNA (10 base pairs). To demonstrate that localization is not due to limitations of the method, a 10 base pair periodic structure of poly(dA)−poly(dT) was created based on the Arnott B-DNA[44] fiber model. Each base pair is rotated by 36° and translated by 3.38 Å; therefore, 10 base pairs complete one full pitch of the double helix and periodicity is inforced in the program. The population densities for the highest occupied molecular orbital (HOMO) and the lowest unoccupied molecular orbital (LUMO) are plotted in Figure 1. As seen from this figure, both the HOMO and LUMO states exhibit very extended and periodic (Bloch-like) states throughout the molecule. No localization is evident.

3.2. Using Classical MD Simulation with an Empirical Force Field to Thermally Sample Poly(dA)−Poly(dT) Configurations. As discussed in the methods section, after an initial equilibration of an explicitly solvated 10-mer B-DNA poly(dA)−poly(dT) with explicit Na^+ ions, production molecular dynamics

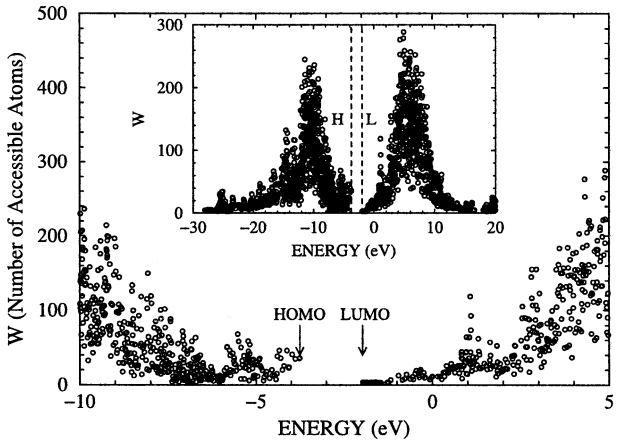

Figure 4. Number of accessible atoms, $W(\nu)$, for each electronic state near the HOMO and LUMO levels. Inset shows number of accessible atoms for all levels. The system contains 10 base pairs of DNA (644 atoms).

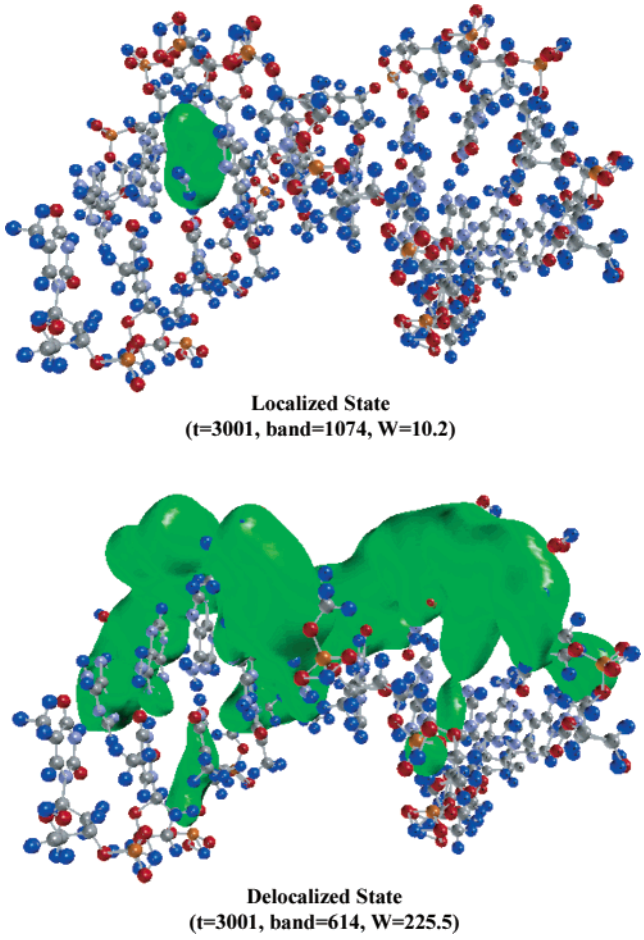

Figure 5. Example of a localized and a delocalized state for two different states in poly(dA)−poly(dT) at time step 3001. For reference, the HOMO is band 1094.

simulations (applying an accurate particle mesh Ewald treatment of the electrostatics) were performed for 10 ns. As shown in Figure 2, a plot of the all-atom root-mean-squared deviation over the entire run is rather stable, and although thermal fluctuations are clearly evident, no large-scale distortions of the structure were observed (beyond sugar repuckering and expected base and backbone fluctuations). A stable portion of the trajectory from 1.5 to 2.5 ns, at 0.5 ps intervals, was analyzed further using the FIREBALL DFT methodology. A straight

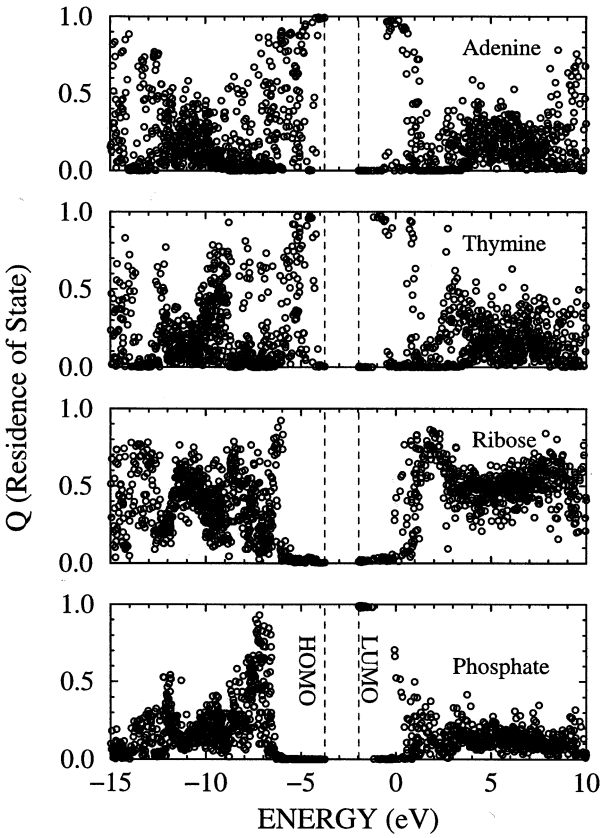

Figure 6. Residence of state gives the location of the wave function for each energy state. States very near the HOMO level are located primarily on the adenine bases. For any given state, the sum of the four residences add to unity.

coordinate averaged structure over this range (1.5−2.5 ns) is only 1.54 Å from the initial canonical B-DNA model.

To give an idea of the range of motion of the configurations sampled in the MD simulation, shown in Figure 3 is a stereoview of representative snapshots from the 1.5−2.5 ns interval. The structures shown were obtained by hierarchically clustering the configurations, based on pairwise RMS deviations, into 10 clusters and then displaying the configuration closest to the centroid of each cluster.

3.3. Electronic States of Configurations Sampled from MD Simulation. We now consider results for a single configuration from the MD simulation (labeled step 3001, the first coordinate set 0.5 ps after a 1.5 ns production simulation). Figure 4 shows the number of accessible atoms, $W(\nu)$, for each electronic state at this time step. It is important to note that near the HOMO and LUMO, the number of accessible atoms is quite small ($\lesssim$30), demonstrating a large degree of localization for the wave functions. This localization extends over several eV and is deeper than just the bandtail states. States further away from the HOMO and LUMO become considerably delocalized, and the number of accessible atoms is much larger. The number of accessible atoms is also small for the lowest energy levels; these deep states consist mainly of 2s levels of oxygen and nitrogen atoms. The degree of localization for two example band states (1074 and 614−larger number implies higher eigenvalue) can be seen in Figure 5 where population density plots of a localized and delocalized state are shown.

As more configurations are analyzed, we see consistently that the number of accessible atoms for the energy levels near the HOMO primarily consist of around 20 atoms. However, as a function of time, different sets of atoms are involved. To determine where the localization occurs, we compute a residence of each state according to the specific DNA component−adenine base, thymine base, ribose backbone, or phosphate group−and determine where the high probability regions are located. Further investigation indicates the residence localization for the highly localized states near the HOMO are contained approximately on single bases in the DNA molecule; adenine for states very near the HOMO and thymine for states slightly lower in energy. This regional population information for the HOMO on adenine

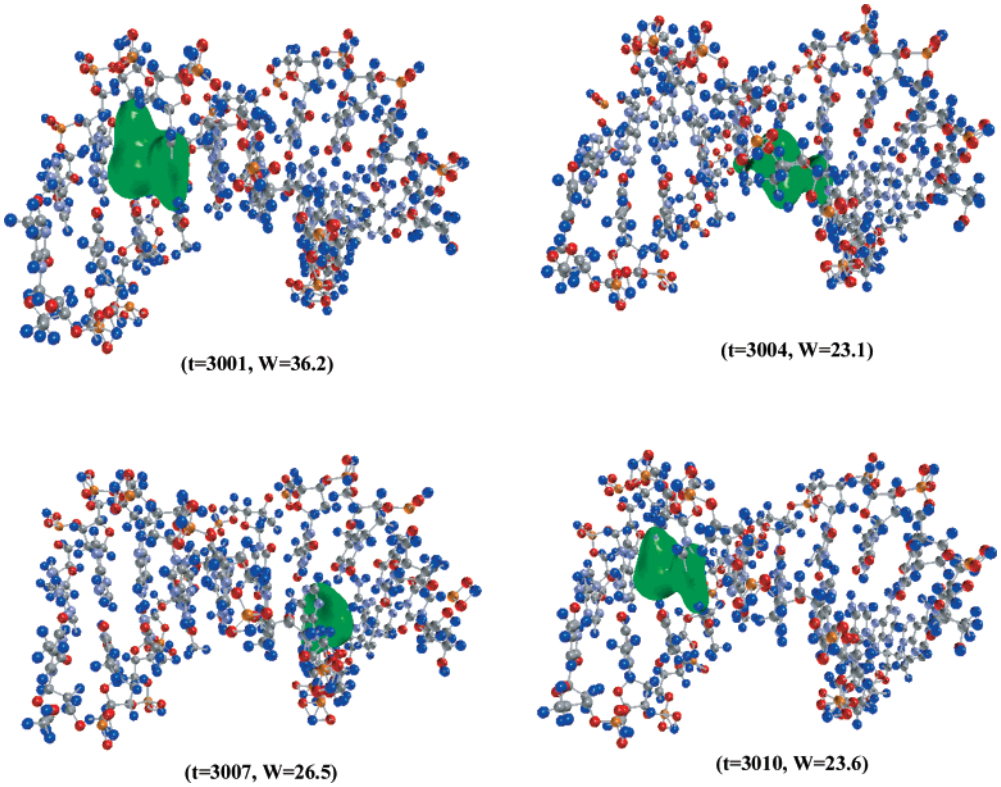

Figure 7. Population density plots for the localized HOMO state as a function of time. The time between snapshots is 1.5 ps.

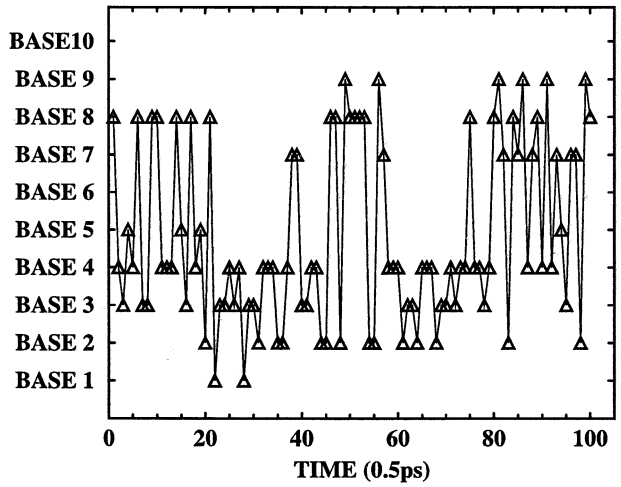

Figure 8. Location of the HOMO as function of time. The 10 bases are the 10 adenine bases on one strand of the DNA. The HOMO is located only on adenine bases.

is plotted in Figure 6. The more extended states (~8 eV to ~18 eV below the HOMO) are found to reside throughout the various DNA components.

As the simulation proceeds in time, the residence of the HOMO level moves from base to base along the poly(dA)−poly(dT) system and large jumps in sequence are possible over this 0.5 ps resolution time scale. This fluctuating residency of the HOMO is visualized in Figure 7, which shows population density plots for a series of snapshots at different times (t = 3001, 3004, 3007, and 3010). The separation between these snapshots is 1.5 ps. Figure 8 shows the location of the HOMO for all 100 snapshots where the electronic structure was calculated in this work. The population is localized on different adenine bases as time progresses and appears to chaotically oscillate between one end of the DNA molecule to the other. The HOMO level's localization on one adenine base is traded for localization on another adenine base through the dynamical simulation. Physically, this trading ought to reflect concerted fluctuations assignable to off-diagonal dynamical disorder in a regular homooligonucleotide duplex. Based on these results, it is conceivable that electron (hole) transfer will occur as two or more localized MO levels are dynamically trading places. Moreover, this swapping may be gated by thermal fluctuations of hydrated counterions, in accordance with the ion-gating transport mechanism proposed in ref 36.

Finally, it is of considerable interest to compare our above results to the known literature data on this theme. Specifically, our findings are in parallel with the most recently established dependence of electronic coupling between DNA bases in the stack on DNA conformational states:[8] a diminuation of the coupling between the DNA purine bases due to the pertinent conformational changes would "arrest" the HOMO at one particular base; whereas, conformationally induced increases in the above coupling ought to promote the "HOMO trading" we revealed here. Our results are also in accordance with the analogous approach put forth most recently in ref 66. To be capable of formulating reasonable suggestions for experimentalists, we would need more detailed calculations not only on poly(dG)−poly(dC) but also on DNA with mixed base sequences.

4. Summary

We present results on the electronic structure of poly(dA)−poly(dT) using our ab initio tight-binding method, called FIREBALL, which is based on norm-conserving pseudopotentials[67,68] and DFT (GGAs). The method scales linearly both with system size and the number of processors, and several thousands of atoms could easily be simulated as the method is shown to be fast and efficient. The results presented here are preliminary results but indicate a marked difference in the nature of the electronic HOMO−LUMO states for the periodic and aperiodic structures of duplex DNA. These results indicate that the HOMO−LUMO states for the periodic structure are quite extended as would be expected for Bloch-like states, while the HOMO−LUMO states for the aperiodic structure demonstrate more localization. The concept of static localization in DNA has previously been considered by Ladik,[41,42] and our results show that such a localization in our structure for aperiodic poly(dA)−poly(dT) DNA reaches far deeper in energy than just the bandtail states.

In conclusion, we observe Anderson localization in DNA which we attribute to the off-diagonal disorder. This disorder results from dynamical variations in DNA intramolecular interactions and coupling of DNA with its environment. These results warrant further investigation, as the role of the dynamical localization may very well suggest an important mechanism of charge transport along the DNA molecule.

Acknowledgment. We thank the following people for their enlightening discussions regarding this ongoing project: David Drabold, Dorian Hatch, Bret Hess, and John Tomfohr. This work was funded in part by NSF DMR-9986706 and by The University of Utah Center for the Simulation of Accidental Fires and Explosions (C-SAFE), funded by the Department of Energy, Lawrence Livermore National Laboratory, under subcontract B341493. Within this DOE funding, allocations of computer time on the SGI Origin 2000 (Nirvana) located at Los Alamos National Laboratory were used in this work; allocations of computer time from the NPACI-SDSC (National Partnership for Advanced Computational Infrastructure−San Diego Supercomputer Center; MCA01S027) and the Center for High Performance Computing at the University of Utah were also used in this work.

References and Notes

(1) Lewis, J. P.; Ordejón, P.; Sankey, O. F. *Phys. Rev. B* **1997**, *55*, 6880−6886.
(2) Dandliker, P. J.; Holmlin, R. E.; Barton, J. K. *Science* **1997**, *257*, 1466−1468.
(3) Beratan, D. N.; Priyadasky, S.; Risser, S. M. *Chem. Biol.* **1997**, *4*, 3−8.
(4) Fink, H. W.; Schoenberger, C. *Nature* **1999**, *398*, 407.
(5) Porath, D.; Bezryadin, A.; Vries, S. D.; Dekker, C. *Nature* **2000**, *403*, 635.
(6) Berlin, Y. A.; Burin, A. L.; Ratner, M. A. *J. Phys. Chem. A* **2000**, *104*, 443−445.
(7) Voityuk, A. A.; Jortner, J.; Bixon, M.; Rösch, N. *Chem. Phys. Lett.* **2000**, *324*, 430−434.
(8) Voityuk, A. A.; Siriwong, K.; Rösch, N. *Phys. Chem. Chem. Phys.* **2001**, *3*, 5421.
(9) Garnier, F.; Korri-Youssoufi, H.; Srivastava, P.; Mandrand, B.; Delair, T. *Synth. Met.* **1999**, *100*, 89.
(10) Yamamoto, T.; Shimizu, T.; Kurokawa, E. *React. Funct. Polym.* **2000**, *43*, 79.
(11) Sies, H. *Mutat. Res.* **1993**, *275*, 367.
(12) Pogozelski, W. K.; Tullius, T. D. *Chem. Rev.* **1998**, *98*, 1089.
(13) Burrows, C. J.; Muller, J. G. *Chem. Rev.* **1998**, *98*, 1109.
(14) Blank, M.; Goodman, R. *IEEE Trans. Plasma Sci.* **2000**, *28*, 168.
(15) Dandliker, P. J.; Nunez, M. E.; Barton, J. K. *Biochemistry* **1998**, *37*, 6491.
(16) Banerjee, S. K.; Christensen, R. B.; Lawrence, C. W.; LeCleric, J. E. *Proc. Nat. Acad. Sci. U.S.A.* **1988**, *85*, 8141.
(17) Taylor, J.-S. *Pure Appl. Chem.* **1995**, *67*, 183.
(18) Dotse, A. K.; Boone, E. K.; Schuster, G. B. *J. Am. Chem. Soc.* **2000**, *122*, 6825.

(19) Eley, D. D.; Spivey, D. I. *Trans. Faraday Soc.* **1962**, *58*, 411.
(20) Okahata, Y.; Kobayashi, T.; Tanaka, K.; Shimomura, M. *J. Am. Chem. Soc.* **1998**, *120*, 6165.
(21) Warman, J. M.; de Haas, M. P.; Rupprecht, A. *Chem. Phys. Lett.* **1996**, *249*, 319.
(22) Aich, P.; Labiuk, S. L.; Tari, L. W.; Delbaere, L. J. T.; Roesler, W. J.; Falk, K. J.; Steer, R. P.; Lee, J. S. *J. Mol. Biol.* **1972**, *294*, 477.
(23) Taubes, G. *Science* **1997**, *275*, 1420.
(24) Ratner, M. *Nature* **1999**, *397*, 480.
(25) Murphy, C. J.; Arkin, M. R.; Jenkins, Y.; Ghatlia, N. D.; Bossman, S. H.; Turro, N. J.; Barton, J. K. *Science* **1993**, *262*, 1025.
(26) Grinstaff, M. W. *Angew. Chem.* **1999**, *111*, 3845.
(27) Schuster, G. B. *Acc. Chem. Res.* **2000**, *33*, 253.
(28) Meggers, E.; Dussy, A.; Schaefer, T.; Giese, B. *Chem. Eur. J.* **2000**, *6*, 485.
(29) Marcus, R. A.; Sutin, N. *Biochim. Biophys. Acta* **1985**, *811*, 265.
(30) Lewis, F. D.; Letsinger, R. L.; Wasielewski, M. R. *Acc. Chem. Res.* **2001**, *34*, 159−170.
(31) Giese, B. *Annu. Rev. Biochem.* **2002**, *71*, 51−70.
(32) Wan, C.; Fiebig, T.; Kelley, S. O.; Treadway, C. R.; Barton, J. K.; Zewail, A. H. *Proc. Nat. Acad. Sci. U.S.A.* **1999**, *249*, 6014.
(33) Reid, G. D.; Whittaker, D. J.; Day, M. A.; Turton, D. A.; Kayser, V.; Kelly, J. M.; Beddard, G. S. *J. Am. Chem. Soc.* **2002**, *124*, 5518−5527.
(34) Robinson, B. H.; Mailer, C.; Drobny, G. *Annu. Rev. Biophys. Biomol. Str.* **1997**, *26*, 629.
(35) Stemp, E. D. A.; Holmlin, R. E.; Barton, J. K. **2000**, *297*, 88.
(36) Barnett, R. N.; Cleveland, C. L.; Joy, A.; Landman, U.; Schuster, G. B. *Science* **2001**, *294*, 567−571.
(37) Anderson, P. W. *Phys. Rev.* **1958**, *109*, 1492−1505.
(38) Dong, J.; Drabold, D. A. *Phys. Rev. Lett.* **1998**, *80*, 1928−1931.
(39) Thomas, P.; Overhof, H.; Kluwer Academic Publisher: Dordrecht, 2001.
(40) Gotze, W. *Philos. Mag. B* **1981**, *43*, 219−250.
(41) Ladik, J.; Seel, M.; Otto, P.; Bakhshi, A. K. *Chem. Phys.* **1986**, *108*, 203−214.
(42) Ye, Y.-J.; Chen, R. S.; Shun, J.; Ladik, J. *Solid State Commun.* **2001**, *119*, 175−180.
(43) Lewis, J. P.; Glaesemann, K. R.; Voth, G. A.; Fritsch, J.; Demkov, A. A.; Ortega, J.; Sankey, O. F. *Phys. Rev. B* **2001**, *64*, 195103.
(44) Arnott, S.; Hukins, D. W. *Biochem. Biophys. Res. Comm.* **1972**, *47*, 1504−1509.
(45) Pearlman, D. A.; Case, D. A.; Caldwell, J. W.; Ross, W. S.; Cheatham, T. E.; Debolt, S.; Ferguson, D.; Seibel, G.; Kollman, P. *Comput. Phys. Comm.* **1995**, *91*, 1−41.
(46) Brooks, B. R.; Bruccoleri, R. E.; Olafson, B. D.; States, D. J.; Swaminathan, S.; Karplus, M. *J. Computat. Chem.* **1983**, *4*, 187.
(47) Aqvist, J. *J. Phys. Chem.* **1990**, *94*, 8021−8024.
(48) Cornell, W. D.; Cieplak, P.; Bayly, C. I.; Gould, I. R.; Merz, K. M.; Ferguson, D. M.; Spellmayer, D. C.; Fox, T.; Caldwell, J. W.; Kollman, P. A. *J. Am. Chem. Soc.* **1995**, *117*, 5179−5197.
(49) Langley, D. R. *J. Biomol. Struct. Dyn.* **1998**, *16*, 487−509.
(50) Hoover, W. G. **1985**, *31*, 1695−1697.
(51) Feller, S. E.; Zhang, Y.; Pastor, W.; Brooks, B. R. *J. Chem. Phys.* **1995**, *103*, 4613−4621.
(52) Ryckaert, J. P.; Ciccotti, G.; Berendsen, H. J. C. *J. Comput. Phys.* **1977**, *23*, 327−341.
(53) Essmann, U.; Perera, L.; Berkowitz, M. L.; Darden, T.; Lee, H.; Pedersen, L. G. *J. Chem. Phys.* **1995**, *103*, 8577−8593.
(54) Beveridge, D. L.; McConnell, K. J. *Curr. Opin. Struct. Biol.* **2000**, *10*, 182−196.
(55) T. E. Cheatham, I.; Kollman, P. A. *Annu. Rev. Phys. Chem.* **2000**, *51*, 435−471.
(56) T. E. Cheatham, I.; Young, M. A. *Biopoly.* **2001**, *56*, 232−256.
(57) Harris, J. *Phys. Rev. B* **1985**, *31*, 1770−1779.
(58) Foulkes, W. M. C.; Haydock, R. *Phys. Rev. B* **1989**, *39*, 12520.
(59) Becke, A. D. **1988**, *38*, 3098−3100.
(60) Lee, C.; Yang, W.; Parr, R. G. *Phys. Rev. B* **1988**, *37*, 785−789.
(61) Lewis, J. P.; Cheatham, T. E.; Starikov, E. B.; Wang, H.; Sankey, O. F. *J. Phys. Chem.* **2002**, submitted.
(62) Hamann, D. R. *Phys. Rev. B* **1989**, *40*, 2980−2987.
(63) Finnis, M. *J. Phys.: Condens. Mater.* **1990**, *2*, 331.
(64) Dornberger, U.; Leijon, M.; Fritzche, H. *J. Biol. Chem.* **1999**, *274*, 6957−6962.
(65) Olson, W. K.; Gorin, A. A.; Lu, X. J.; Hock, L. M. *Proc. Natl. Acad. Sci. U.S.A.* **1998**, *95*, 11163−11168.
(66) Troisi, A.; Orlandi, G. *J. Phys. Chem. B* **2002**, *106*, 2093−2101.
(67) Hamann, D. R.; Schlüter, M.; Chiang, C. *Phys. Rev. Lett.* **1979**, *43*, 1494−1497.
(68) Bachelet, G. B.; Hamann, D. R.; Schlüter, M. *Phys. Rev. B* **1982**, *26*, 4199−4228.